



Cite this: *Green Chem.*, 2025, **27**, 4267

## A closed-loop zero-liquid-discharge process for the precipitative separation of all valuable metals from waste lithium-ion batteries of mixed chemistries at room-temperature†

Nishu Choudhary,<sup>‡<sup>a,d</sup></sup> Hiren Jungi,<sup>‡<sup>b,d</sup></sup> Maulik V. Gauswami,<sup>‡<sup>a</sup></sup> Anu Kumari,<sup>a</sup> Arvind B. Boricha,<sup>\*<sup>b</sup></sup> Jatin R. Chunawala,<sup>c,d</sup> Joyeemitra<sup>\*<sup>b,d</sup></sup> and Alok Ranjan Paital <sup>‡<sup>a,d</sup></sup>

Recycling spent lithium-ion batteries (LIBs) and recovering valuable metals is essential for resource sustainability, minimizing environmental footprint, and maximizing resource utilization. However, many existing recycling methods are costly, energy-intensive, pose fire hazards due to organic solvents, or generate extensive secondary waste. Also, most studies have focused on metal recovery from simple cathode materials, such as LCO batteries, with less attention on mixed LIBs, containing multiple metals. To address these concerns, we have developed a room-temperature leaching process for NMC-type cathode materials that shows high leaching efficiency for Li, Co, Ni, and Mn (~98%) under optimized conditions of 4 M acetic acid, 5 vol% H<sub>2</sub>O<sub>2</sub>, 20 g L<sup>-1</sup> pulp density in a duration of 5 h. We have also developed a downstream process that enables the sequential and selective precipitation of all metals through judicious control of the solution pH and using specific reagents. As a result, all metal salts (Ni(DMG)<sub>2</sub>, Co<sub>3</sub>S<sub>9</sub>, Mn(OH)<sub>2</sub>, and Li<sub>2</sub>CO<sub>3</sub>) were recovered in pure form ( $\geq 98\%$ ) with high recovery efficiencies (85–99%). Additionally, excess acetic acid and the by-product sodium acetate (purity  $\geq 97\%$ ) are also recovered, establishing a zero liquid discharge process. We also recycled Ni(DMG)<sub>2</sub> complex to recover  $\beta$ -Ni(OH)<sub>2</sub> and DMG for re-use. Furthermore, the recovered acetic acid was used to recover lithium, copper, and graphite from the anode material. This process offers several advantages over existing technologies, including low energy requirements for a room temperature process, eliminating cathode pre-treatment, the use of selective precipitation methods that preclude the necessity for organic solvents, and fire hazards. This environment-friendly zero-liquid discharge process offers a sustainable pathway for LIB recycling.

Received 5th January 2025,  
Accepted 19th March 2025

DOI: 10.1039/d5gc00054h  
rsc.li/greenchem

### Green foundation

1. This study presents an environmentally friendly hydrometallurgical leaching process using acetic acid at room temperature & subsequent separation of metal salts solely through precipitation methods from spent LIBs.
2. The process eliminates the necessity for elevated temperatures and organic solvents, thereby reducing environmental and fire hazards associated with handling bulk organic solvents. The excess lixiviant (acetic acid) and the by-product (sodium acetate) are recovered in the process, achieving a zero liquid discharge (ZLD) process.
3. Future studies will be conducted to improve the pulp density during leaching in order to reduce acid consumption, as well as to develop a continuous process at a larger scale for industrial viability.

<sup>a</sup>*Salt and Marine Chemicals Division, CSIR-Central Salt & Marine Chemicals Research Institute, G.B. Marg, Bhavnagar-364002, Gujarat, India.*

*E-mail: arpaitha@csmcri.res.in, alokpaitha@gmail.com*

<sup>b</sup>*Inorganic Materials & Catalysis Division, CSIR-Central Salt & Marine Chemicals Research Institute, G.B. Marg, Bhavnagar-364002, Gujarat, India.*

*E-mail: abboricha@gmail.com, joyeemitra@csmcri.res.in, joyeemitra@gmail.com*

<sup>c</sup>*Process Design and Engineering Division, CSIR-Central Salt & Marine Chemicals Research Institute, G.B. Marg, Bhavnagar-364002, Gujarat, India*

<sup>d</sup>*Academy of Scientific and Innovative Research (AcSIR), Ghaziabad-201002, India*

† Electronic supplementary information (ESI) available. See DOI: <https://doi.org/10.1039/d5gc00054h>

‡ These authors contributed equally.

## Introduction

There is a global drive to upcycle and recycle various waste materials generated in our daily lives, with the aim of minimizing waste generation and reducing pollutant accumulation.<sup>1–3</sup> In this context, the global thrust towards a low-carbon/carbon neutral energy scenario is fuelling the ever-increasing demand for rechargeable lithium-ion batteries (LIBs), which offer advantages of high energy density, prolonged storage capacity, compact size, and large shelf life while mitigating greenhouse gas emissions.<sup>4,5</sup> This has resulted in its overwhelming popularity for applications in portable electronic devices, and also the global revolution of electric vehicles (EVs).<sup>6</sup> However, the average cycle life of these LIBs is about 5–10 years, resulting in the accumulation of massive volumes of spent LIBs, with an estimated amount of 21 million battery packs of spent LIBs from EVs alone.<sup>7</sup> The development of recycling strategies for spent LIBs is essential not only from an environmental point of view to minimize waste accumulation, but also to maximize resource conservation to ensure a smooth supply of elements for battery manufacturers. Additionally, it ensures a distribution of critical resources without geopolitical constraints. Efficient and complete recycling is expected to reduce the requirement of mined lithium to ~37%, and substantially reduce the necessity of Co, the most expensive component, mined from potentially conflict-torn zones.<sup>6,8</sup> Consequently, the recycling of spent LIBs has gained considerable attention and has been the subject of numerous studies.<sup>4,9</sup> Despite this, existing technologies face several challenges from a practical standpoint.<sup>9,10</sup>

In spent LIBs, the cathode has the maximum recoverable value, and the cathode active materials *i.e.* LiCoO<sub>2</sub> (LCO), LiNiO<sub>2</sub> (LNO), LiMn<sub>2</sub>O<sub>4</sub> (LMO), LiNi<sub>x</sub>Co<sub>y</sub>Mn<sub>z</sub>O (NCM), *etc.* are processed *via* different approaches including direct recycling, pyrometallurgy, hydrometallurgy, bioleaching, or a combination thereof.<sup>11–15</sup> Energy-intensive pyrometallurgical processes are industrially preferred to extract a specific metal, despite the release of toxic gaseous fumes causing subsequent pollution.<sup>12,16</sup> Hydrometallurgy is a more viable option owing to a high metal recovery rate and purity of the product.<sup>17,18</sup> Hydrometallurgy often involves time-consuming pre-treatment steps to separate the cathode active material (black mass) from aluminium foil by either heating at elevated temperatures or by chemical treatment,<sup>19,20</sup> followed by toxic, corrosive acid or alkali treatment to maximize metal leaching.<sup>9,21–25</sup> Organic acids including malic acid, formic acid, ascorbic acid, citric acid, *etc.* have emerged as environmentally benign alternatives compared to mineral acids and alkalis, but their high cost often hinders their extensive applications.<sup>11,26,27</sup> Researchers have explored greener alternatives such as triethyl phosphate (TEP) as replacements for organic solvents like dimethylformamide (DMF), and *N*-methylpyrrolidone (NMP) to dissolve the PVDF binder to separate the black mass from aluminium foil, but the process required large amounts of organics, which poses significant fire hazards.<sup>28</sup> Selective extraction of metals in the presence of organic solvent followed by chemical pre-

cipitation has also gained significant attention in recent years, to circumvent the use of mineral acids. Cyanex 272 is specific to cobalt and effectively separates cobalt and nickel,<sup>21,29</sup> while di(2-ethylhexyl)phosphoric acid (D2EHPA) has been reported to extract copper and manganese with >98% extraction rates.<sup>30</sup> The solvent extraction method is beneficial for obtaining high-purity products, but the method is encumbered due to high expenses, toxicity, and potential fire hazards.<sup>31</sup> In recent times, ionic liquids (ILs) and deep eutectic solvents (DES) have gained significant attention as green solvents for efficient leaching, as their acidity, reducibility, and coordination properties can be tuned to effectively separate valuable metals from the spent LIBs.<sup>32,33</sup> While many studies have demonstrated success with LCO batteries,<sup>6,34–38</sup> less attention is given to the more challenging NCM-type cathode materials, which contain multiple metals. Although ILs and DES are considered green solvents, their synthesis often involves multiple steps with significant chemical wastage<sup>39</sup> and their slow degradation can result in accumulation in the environment, causing pollution by either the solvents or their metabolites.<sup>40</sup> However, the extent of their environmental impact remains unclear.<sup>39</sup> While DES are simpler to synthesize than ILs, they are sometimes reported to show higher toxicity than their individual components.<sup>41</sup> Additionally, their use on an industrial scale requires high concentrations and elevated temperature, raising both toxicity and economic concerns.<sup>38</sup> In many instances, elevated temperatures and concentrations of lixivants & reducing agents are preferred for maximizing leaching efficiency.<sup>42,43</sup> However, these conditions have drawbacks, such as the decomposition of reducing agents into toxic gases, higher reagent dosages, and increased resource consumption. Therefore, processes that operate at lower temperatures or without external heat supply, albeit rarely explored in the contemporary literature, are vital for energy efficiency and reducing reagent consumption.<sup>44,45</sup> The downstream separation of individual metals from the leached liquor involves precipitation, solvent extraction or a combination thereof, depending on the number of metal ions present and the requirement of individual metal or mixed metal compositions. The separation of individual metals from mixed-type batteries having multiple metals poses challenges due to the presence of several interfering metal ions and increases the number of operating steps. A recent report discusses alkali treatment to remove transition metals as mixed metal hydroxide precipitate, effectively separating lithium, which can be recovered from the filtrate.<sup>46</sup> While precipitation methods are known for separating metal ions, they are primarily applied to leachates containing fewer metal ions.<sup>47,48</sup> The separation of individual metals from cathodes having mixed chemistries with interfering multiple metal ions is challenging during selective precipitation. Despite the challenges, the separation of individual metals from mixed-type cathodes is imperative as it facilitates industrial adaptation and broadens the scope of utilization of the metals thereby improving the overall process economy.<sup>49,50</sup>

A comprehensive literature analysis reveals several limitations in the existing processes: (i) recycling of spent cathodes

do not typically involve batteries having mixed chemistries including NCM, hindering a comprehensive understanding of the challenges associated with metal recovery in the presence of mixed cathode materials;<sup>51</sup> (ii) pre-treatment of cathode to remove PVDF binder by heat treatment that generate hazardous hydrogen fluoride gas, or require organic solvents to dissolve the binder and separate the black mass from aluminium foil; (iii) majority of leaching processes are conducted at elevated temperatures and require organic solvents for metal extraction, with potential to cause fire hazard and generating secondary waste; (iv) contemporary literature rarely addresses the recovery of excess lixiviant, reagents used for selective precipitation and by-products, thus failing to achieve a zero-liquid discharge process, which is becoming increasingly relevant considering the prevalent environmental norms.

To overcome these limitations, and in order to develop a recycling protocol along the lines of green chemistry principles, we have developed a room-temperature leaching process using the whole cathode of mixed chemistries without any pre-treatment step, using acetic acid that simultaneously separates out the aluminium foil during leaching. A sustainable downstream process was developed for the selective sequential precipitation of individual metals, precluding the necessity of organic solvents in the metal separation processes, to minimize fire hazards associated with recycler industries. The excess lixiviant and by-product of the process was also recovered, resulting in a zero-liquid discharge process. The main findings of this research are the following: (i) a pre-treatment free leaching process that is effective for the recycling of cathodes of mixed chemistries without any external heating; (ii) A selective sequential precipitation route to recovery individual metals without organic solvent extraction steps; (iii) recovery of excess acetic acid, and byproduct sodium acetate culminating in a zero-liquid discharge process, and (iv) the reuse of recovered lixiviant for the recovery of lithium, copper and graphite from anode, and the recovery, reuse of reagents used in metal precipitation. Thus, this work is a step towards a sustainable and economical process to recover metals from the spent cathode of LIBs, minimizing adverse environmental footprint.

## Results & discussions

### Leaching studies

The mixed mobile batteries were discharged and disassembled manually to separate the cathode, anode, metal casings, and plastic separators (Fig. S1,† detailed procedure in ESI†). The whole cathode, which is aluminium foil with cathode active

material, was heated in air at 450 °C for 5 h to remove the binder. The cathode powder was scrapped and removed to determine its composition by digesting it in aqua-regia, followed by ICP-MS analysis as shown in Table 1. This scrapped cathode powder was then used in leaching studies and optimization. We selected hydrogen peroxide as the reducing agent considering its extensive use in industrial processes, and its decomposition into water & oxygen without introducing any impurities into the system.<sup>52</sup> Similarly, acetic acid is used as the environmentally friendly lixiviant, any excess of it being recoverable through distillation, and in view of prior reports of its use for the treatment of ore and scraps containing transition metals.<sup>53,54</sup> The powder XRD characterization of cathode powder indicates a blend of LCO, LMO and NCM-type cathode material, supporting the ICP-MS analysis results (Fig. 1). During the leaching process in acetic acid, the high valence transition metal ions tend to reductively dissolve in the presence of hydrogen peroxide (H<sub>2</sub>O<sub>2</sub>). The reactions between the cathode powder with acetic acid and H<sub>2</sub>O<sub>2</sub> are presented below:

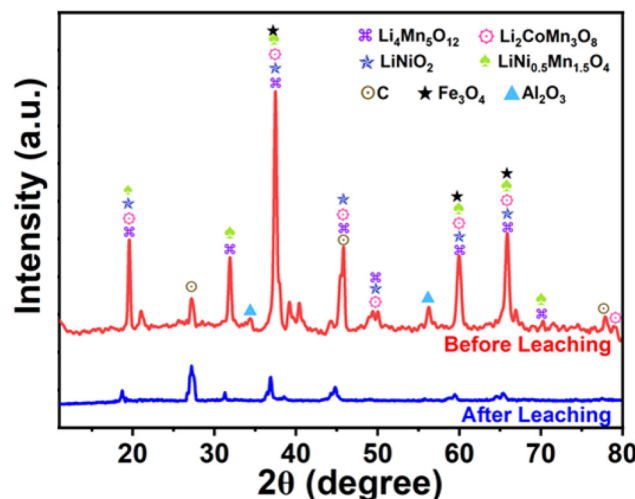
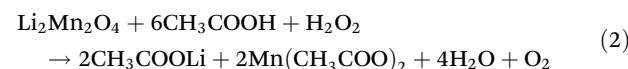
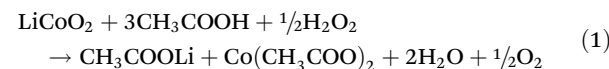
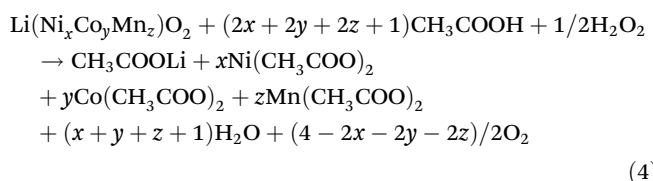
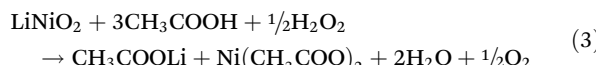


Fig. 1 Powder XRD pattern of cathode powder before and after leaching.

Table 1 The average metallic composition of mixed cathodes of spent LIBs

| Samples  | Li                     | Co                     | Ni                     | Al                     | Mn                     |
|--|------------------------|------------------------|------------------------|------------------------|------------------------|
| Elements (wt (%)) in cathode powder (digested in aqua-regia)                                       | 5.2%                   | 28%                    | 3%                     | —                      | 6%                     |
| Leaching solution of cathode powder (optimized condition; pulp density: 20 g L <sup>-1</sup> )     | 1.03 g L <sup>-1</sup> | 5.49 g L <sup>-1</sup> | 0.59 g L <sup>-1</sup> | —                      | 1.19 g L <sup>-1</sup> |
| Leaching solution of whole cathode (with Al foil; 1 kg scale; pulp density: 20 g L <sup>-1</sup> ) | 0.86 g L <sup>-1</sup> | 5.02 g L <sup>-1</sup> | 0.54 g L <sup>-1</sup> | 0.45 g L <sup>-1</sup> | 1.06 g L <sup>-1</sup> |



The leached liquor under optimized conditions (discussed later) shows a leaching efficiency  $\geq 98\%$  for all metal ions, also supported by diminished peaks in PXRD (Fig. 1 and Table 1). Once the optimal conditions were determined, the entire cathode (including Al foil) was cut into small pieces and used for 1 kg scale leaching studies. The direct use of the whole cathode offered the advantage of avoiding additional pre-treatment steps involving organic solvents and calcination at elevated temperatures, thus saving time and reducing energy consumption. During the whole cathode leaching, it was observed that the Al foil separated effectively with concurrent leaching of metal ions. After filtration, the minor undissolved fine residue was separated effectively from Al foil by simply sieving. It is observed that by using the whole cathode, some amount of Al is leached into the leached liquor, which was subsequently utilized for sequential separation of metal ions.

### Optimization of leaching parameters

The initial leaching experiment was conducted at room temperature considering the exothermic nature of the reaction

while using  $\text{H}_2\text{O}_2$ . A typical reaction condition of 3 M acetic acid, 20 g  $\text{L}^{-1}$  solid–liquid ratio, 7.5 vol%  $\text{H}_2\text{O}_2$  for 7 h gives a leaching efficiency  $\geq 78\%$  for all metal ions. To investigate the impact of temperature on these extraction processes, the temperature was varied from room temperature ( $30\text{ }^\circ\text{C}$ , without external heating) to  $90\text{ }^\circ\text{C}$ , while maintaining the other parameters constant. It is observed that the metal leaching efficiency decreased with an increase in the reaction temperature, probably due to the faster decomposition of  $\text{H}_2\text{O}_2$  at higher temperatures (Fig. 2A). Notably, due to the exothermic nature of the reaction, the actual temperature of the reaction medium reached  $65\text{ }^\circ\text{C}$  without any external heating at room temperature, which facilitated metal leaching. Similarly, external heating *i.e.* maintaining the heater temperature at  $70\text{ }^\circ\text{C}$  and  $90\text{ }^\circ\text{C}$  raised the suspension temperature to  $90\text{ }^\circ\text{C}$  and  $110\text{ }^\circ\text{C}$ , respectively. Higher temperatures enhanced the decomposition of  $\text{H}_2\text{O}_2$  into water, leading to a reduced extraction efficiency, often necessitating a greater amount of  $\text{H}_2\text{O}_2$  to maintain an extraction efficiency comparable to the room temperature experiments. However, increased levels of  $\text{H}_2\text{O}_2$  can also be harmful to the process, as there are reports indicating that heat sources and impurities such as acids and metallic ions can trigger the explosive breakdown of peroxides, potentially causing fires.<sup>55</sup> Ascertaining that room temperature (absence of external heating) is most suited for the leaching of metals from the spent cathode, we focused on optimizing the other parameters. The solid-to-liquid ratio (S/L) was varied between 20 g  $\text{L}^{-1}$  to 100 g  $\text{L}^{-1}$  to examine its effect on leaching efficiency under the above-mentioned leaching conditions. It is observed that an increased S/L ratio has an unfavorable

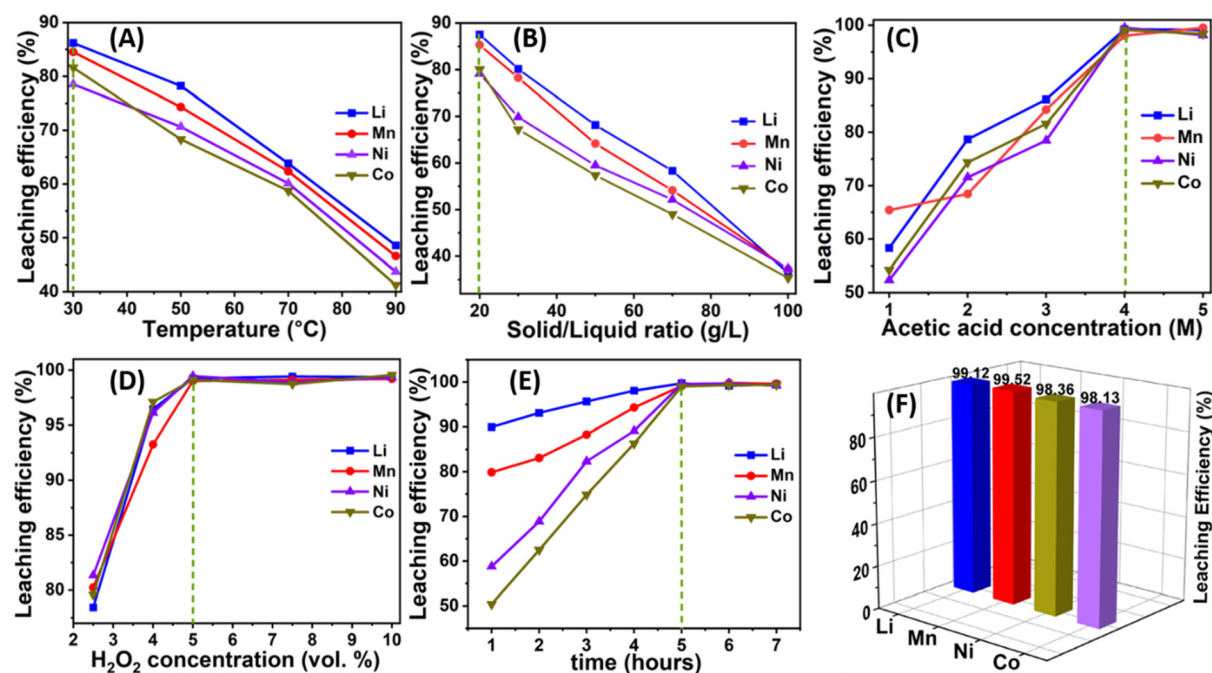


Fig. 2 The effects of (A) reaction temperature, (B) pulp density, (C) acid concentration, (D)  $\text{H}_2\text{O}_2$  dosage, (E) leaching time, and (F) leaching efficiencies of metals under optimized conditions.

effect on metal extraction, as the efficiency of metal extraction decreased with the increase in S/L ratio (Fig. 2B). Subsequently, 20 g L<sup>-1</sup> was established as the optimal S/L ratio for further investigation.<sup>47</sup> A small S/L ratio is considered beneficial to maximize leaching, as the surface area available per unit volume is high, while practically, a high S/L ratio is preferred for a high process throughput at the cost of leaching efficiency.<sup>20,21</sup> The acetic acid concentration was subsequently varied from 1 M to 5 M keeping the other parameters constant (20 g L<sup>-1</sup> solid–liquid ratio, 30 °C, 7.5 vol% H<sub>2</sub>O<sub>2</sub> & 7 h). It is observed that the efficiency of metal extraction increased up to an acid concentration of 4 M, beyond which it reached a plateau with minimal observable changes (Fig. 2C). Consequently, the remaining parameters were sequentially optimized, with the acetic acid concentration set at 4 M. Then the H<sub>2</sub>O<sub>2</sub> concentration was varied from 2.5 to 10 vol% while keeping the other parameter fixed (4 M acid, 20 g L<sup>-1</sup> S/L ratio, 7 hour time, 30 °C). It is observed that the extraction efficiency of metals increased up to an H<sub>2</sub>O<sub>2</sub> concentration of 5 vol%, and a further increase in H<sub>2</sub>O<sub>2</sub> did not significantly improve the leaching efficiency (Fig. 2D). It is well known that H<sub>2</sub>O<sub>2</sub> helps in the reductive dissolution of metals, where the high valence transition metals were reduced to their lower valent states and simultaneously escalating the lithium leaching. Consequently, an H<sub>2</sub>O<sub>2</sub> concentration of 5 vol% was identified as optimal for subsequent investigations. Finally, the leaching time was varied from 1 to 7 hours while maintaining other conditions constant (4 M acetic acid, 20 g L<sup>-1</sup> pulp density, 5% H<sub>2</sub>O<sub>2</sub> (v/v), and a leaching temperature of 30 °C). It is observed that the leaching efficiency of metals increased up to 5 hours, beyond which negligible changes were observed (Fig. 2E). Accordingly, a leaching time of 5 hours was selected as the optimal duration. Based on the aforementioned experiments, room temperature (30 °C), 20 g L<sup>-1</sup> pulp density, 4 M acetic acid, 5 vol% H<sub>2</sub>O<sub>2</sub>, and a time duration of 5 h was determined as the optimal parameters for achieving a >98% leaching efficiency of metals (Fig. 2F). Under this leaching condition, a 1 kg batch of whole cathode (with Al foil) (total 50 L: 2.5 L H<sub>2</sub>O<sub>2</sub> & 47.5 L of 4 M acetic acid) used for leaching showing concurrent leaching of metals and separation of undissolved Al foil avoiding pre-treatments (Table 1). The leached liquor from the whole cathode was processed in 1 L batches for selective & sequential precipitation of metals.

### Exploration of the leaching kinetics

Exploration of leaching kinetics for the dissolution of cathode material from spent LIBs in the lixiviant is crucial in maximizing the leaching efficacy of the system. Metal leaching from the spent cathode of LIBs is a heterogeneous solid–liquid process occurring on the outer surface of the unreacted black mass particles. This entails a reduction in the volume of the particles owing to the gradual dissolution of the lithiated metal oxides in the solution. Hence, the shrinking core model (SCM) was utilized to probe the kinetics of metal leaching

from used LIBs.<sup>56</sup> The equations governing the steps in the SCM model are detailed below:

$$X = kt \quad (5)$$

$$1 - (1 - X)^{1/3} = kt \quad (6)$$

$$1 - 2X/3 - (1 - X)^{2/3} = kt \quad (7)$$

In these equations,  $X$  denotes the leaching efficiency, and  $k$  represents distinct process-controlled rate constants at time  $t$ . This model delineates the progression where the unreacted core undergoes reduction and dissolution (controlled by the mass transfer process in the liquid layer, eqn (5)), with the chemical reaction on the surface (eqn (6)) and the internal diffusion in the residual layer (eqn (7)) typically governing the rate during leaching. Upon careful examination of these kinetic equations governing the metal leaching process from cathode powder, it becomes evident that the surface chemical reaction control model aligns effectively with the observed data. With the increase of H<sub>2</sub>O<sub>2</sub>, a noteworthy reductive transformation of metals such as Co<sup>3+</sup> and Mn<sup>4+</sup> occurs, resulting in more soluble Co<sup>2+</sup> and Mn<sup>2+</sup> species. The leaching data collected at varying temperatures was fitted with different kinetic equations. The data for mass transfer corresponding to eqn (5) revealed an increase in leaching efficiency over time, as depicted in (Fig. S2†). The leaching data indicated an excellent fit to eqn (6) and (7) ( $R^2$  values >0.95), and are illustrated in (Fig. 3) and (Fig. S3†) respectively. This suggests that both the processes of diffusion through the layers of residue and the chemical reactions occurring at the surface are pivotal in the leaching process. To determine the apparent activation energies ( $E_a$ ) for the metals during the leaching process, the Arrhenius equation ( $\ln k = \ln A - E_a/RT$ ) was employed, where  $k$  is the rate constant,  $A$  is the frequency factor,  $R$  is the gas constant, and  $T$  is the temperature. The plot between  $\ln k$  and  $1/T$  from the slopes obtained from (Fig. 3) provides a superior fit for the observed dissolution kinetics, as shown in eqn (6) in (Fig. S4†). As the leaching process involving H<sub>2</sub>O<sub>2</sub> reductant is exothermic, the rate constant decreases with an increase in temperature. The apparent activation energies were determined to be 26 kJ mol<sup>-1</sup>, 27 kJ mol<sup>-1</sup>, 32 kJ mol<sup>-1</sup>, and 37 kJ mol<sup>-1</sup> for Li, Mn, Ni, and Co respectively, from the graph of  $\ln k$  versus  $1/T$ . These negative values are deemed physically insignificant and indicate that leaching efficiency diminishes with an increase in temperature above 60 °C.<sup>27</sup>

### Selective and sequential precipitation for the recovery of metals from the leached liquor

After the leaching of valuable metal ions upon treatment with the lixiviant acetic acid, it is important to recover the metal ions in pure form. The leaching solution obtained after the reductive leaching of Li, Ni, Co, and Mn was utilized for the selective, sequential recovery of the constituent metals. There are various methods reported in the literature such as solvent extraction, precipitation, and a combination of solvent extraction followed by precipitation. Among these methods, sequen-

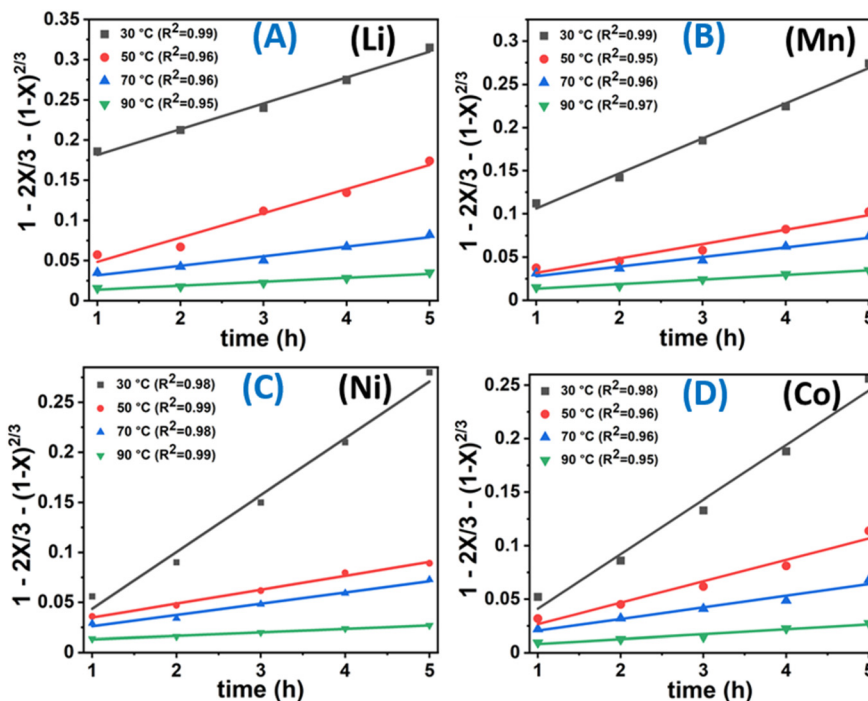


Fig. 3 (A) Plot between  $1 - 2X/3 - (1 - X)^{2/3}$  versus time (h) for Li, (B) Mn, (C) Ni, and (D) Co under optimized conditions ( $S\text{ L}^{-1}$  ratio:  $20\text{ g L}^{-1}$ ;  $\text{H}_2\text{O}_2$  conc: 5%; acetic acid conc: 4 M; time: 5 h) varying temperature.

tial & selective chemical precipitation is advantageous as it precludes the use of organic solvents, thereby minimizing fire hazard and also reducing the number of processing steps compared to solvent extraction. However, selective precipitation of individual metals from batteries of mixed metal-based composition including NCM-type cathodes is challenging due to the interference of metal ions and is rarely attempted in the literature. Though some literature has shown pH-controlled selective precipitation from binary mixtures, achieving the individual metal separation in pure form is challenging in the presence of complex mixtures. Considering the complexity of the system, the leached liquor was treated with various chemical reagents sequentially at appropriate pH for selective precipitation of metal ions, to ensure the generation of a single by-product, which could be separated at the end of the process. Initially, dimethyl glyoxime (DMG), known for its affinity for Ni, was added in the mixed metal containing leached liquor to separate out the highly insoluble  $\text{Ni}(\text{DMG})_2$  complex (yield = 99.32%) selectively,<sup>31</sup> based on  $K_{\text{sp}}$  ( $2.1 \times 10^{-24}$ ) value. It is observed that cobalt does not yield any precipitate with DMG in acetic acid medium ( $\text{pH} \sim 3.5$ ). The purity of the recovered  $\text{Ni}(\text{DMG})_2$  complex was established from the powder XRD (Fig. 4A).<sup>57</sup> The FT-IR peaks corresponding to the  $\nu_{\text{C}=\text{N}}$  stretching vibration in  $(\text{DMG})_2$  complex were observed at  $1571\text{ cm}^{-1}$ , while the vibrations due to N-OH bending appeared at  $1364\text{ cm}^{-1}$ . Peaks at  $1240\text{ cm}^{-1}$  and  $1101\text{ cm}^{-1}$  were accounted for by the N-O  $\nu_{\text{symm}}$  and  $\nu_{\text{asymm}}$  stretching vibrations, respectively, formed upon coordination of the N-OH group with  $\text{Ni}^{2+}$ . Additionally, the  $987\text{ cm}^{-1}$  peak corresponded to C-C bonds,

while peaks at  $743\text{ cm}^{-1}$  and  $518\text{ cm}^{-1}$  were indicative of N-Ni bond (Fig. S5A†). The FESEM image of  $\text{Ni}(\text{DMG})_2$  complex revealed a rectangular belt-like morphology (Fig. 4D). EDX elemental mapping confirmed the presence of Ni, C, O, and N, with no other transition metal ions, affirming the purity of the product (Fig. S5B†). Finally, ICP-MS analysis of the acid-digested solution corroborated the presence of only nickel with a purity of  $99 \pm 0.26\%$ . The  $\text{Ni}(\text{DMG})_2$  complex was further recycled to get  $\beta\text{-Ni(OH)}_2$  and DMG, which was reused in subsequent cycles of Ni recovery from used LIBs (discussed in subsequent sections). After the separation of nickel, the pH of the solution was  $\sim 3.7$ , and considering the low solubility of cobalt sulfides in acidic solutions, and less interference from manganese in acetic acid medium, cobalt was separated as cobalt sulfide ( $K_{\text{sp}} \sim 3 \times 10^{-26}$ ).<sup>47</sup> A quantitative  $\geq 99\%$  recovery with high purity of cobalt sulfide was observed. The PXRD pattern of the precipitated cobalt sulfide suggested an amorphous nature with broad peaks, indicating a probable composition of  $\text{Co}_9\text{S}_8$  (JCPDS no. 86-2273) (Fig. 4B) and also supported by FTIR stretching frequency values  $\sim 1074\text{ cm}^{-1}$  corresponding to C=S stretching, and  $603\text{ cm}^{-1}$  ascribed to the tensile vibration of  $\text{Co}_x\text{S}_y$  (Fig. S6A†). Calcination improved the crystallinity of the sample, possibly by removing the traces of carbon and oxygen attributed to the adhered acetate, further confirming the identity of the material as  $\text{Co}_9\text{S}_8$ . SEM images revealed a spheroidal morphology of the  $\text{Co}_9\text{S}_8$  particles (Fig. 4E), while EDX elemental mapping confirmed the presence of Co and S without any other metallic impurities (Fig. S6B†). ICP-MS results indicated the absence of other

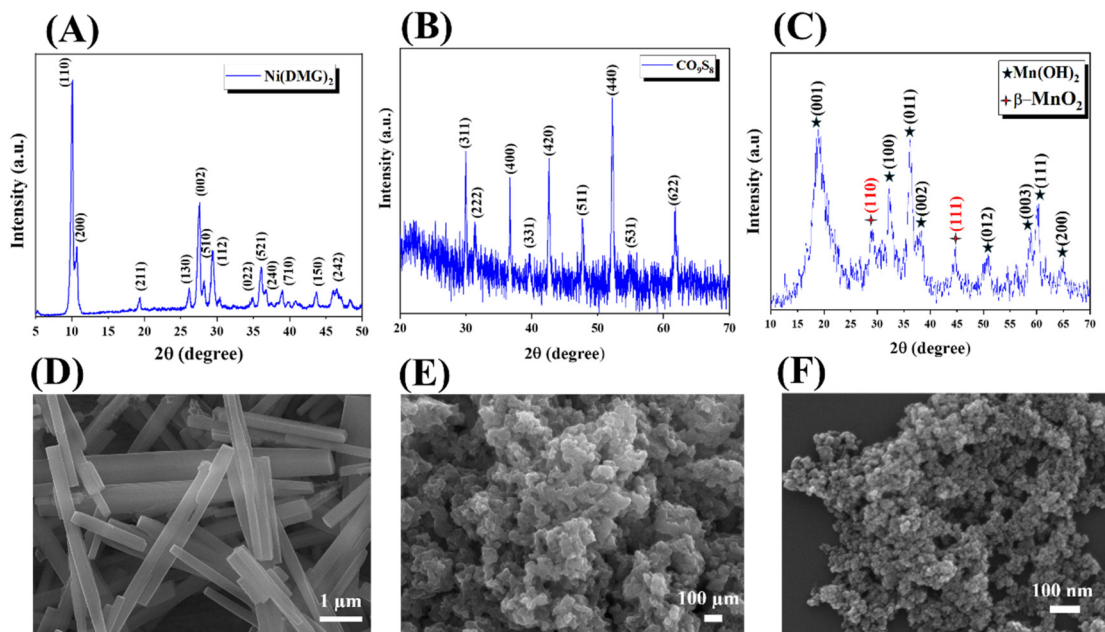


Fig. 4 Powder XRD of (A) Ni(DMG)<sub>2</sub> (B) Co<sub>9</sub>S<sub>8</sub> (C) Mn(OH)<sub>2</sub>. FE-SEM morphology (D) Ni(DMG)<sub>2</sub> (E) Co<sub>9</sub>S<sub>8</sub> (F) Mn(OH)<sub>2</sub>.

metallic impurities, demonstrating a purity of  $98 \pm 0.56\%$ . After the cobalt removal, the separation and precipitation of manganese and lithium were attempted under basic conditions. Therefore, instead of neutralization of excess acid with the addition of chemicals, the recovery of excess lixiviant acetic acid was attempted at this stage, *via* vacuum distillation (Fig. 8). This endeavor of recovering the excess acetic acid was undertaken from the economic and sustainability standpoint, in order to reduce the chemical composition, minimizing potential sources of waste and to make the process more cost competitive. After recovering the acetic acid, the residual mass was dissolved in water and NaOH was added to separate aluminium and manganese as their hydroxides up to pH  $\geq 12$ . Aluminium could be separated first within the pH range of 4–6, followed by the precipitation of manganese as Mn(OH)<sub>2</sub> (recovery  $\geq 99\%$ ). Considering the small amount of aluminium, and the fact that neither aluminium nor manganese as hydroxides has much commercial value, these could be precipitated together by raising the pH up to  $\sim 12$ , thereby reducing the number of steps. The PXRD pattern indicated a crystalline nature with broad peaks of Mn(OH)<sub>2</sub> (JCPDS no. 73-1604), in addition to minor peaks ascribed to the surface oxidation of a small amount of Mn(OH)<sub>2</sub> to  $\beta$ -MnO<sub>2</sub>. This finding was also supported by SEM images (Fig. 4C and F). EDX elemental mapping showed the presence of Mn and O, without any other metallic impurities (Fig. S7†). ICP-MS results confirmed the absence of other metallic impurities with a purity of  $98.5 \pm 0.74\%$ . After the separation of Mn(OH)<sub>2</sub>, the mother liquor was treated with excess Na<sub>2</sub>CO<sub>3</sub> or Na<sub>3</sub>PO<sub>4</sub> in boiling water to isolate lithium as Li<sub>2</sub>CO<sub>3</sub> or Li<sub>3</sub>PO<sub>4</sub>, which were filtered hot and washed with hot water, in an attempt to maximize lithium recovery and enhance its purity. The FT-IR spectrum of recov-

ered Li<sub>2</sub>CO<sub>3</sub> depicted a peak of  $\sim 498\text{ cm}^{-1}$  indicating the presence of Li–O vibration, in addition to a doublet peak of  $\sim 1425\text{--}1490\text{ cm}^{-1}$  (Fig. S8A†). The PXRD patterns of both indicated a crystalline nature (JCPDS no. 29-0801 & JCPDS no.: 84-0046 for Li<sub>2</sub>CO<sub>3</sub> & Li<sub>3</sub>PO<sub>4</sub> respectively) (Fig. 5A and B). Morphological analysis using FESEM revealed rod-like morphology for Li<sub>2</sub>CO<sub>3</sub> and spheroidal morphology of Li<sub>3</sub>PO<sub>4</sub> (Fig. 5C and D). EDX elemental mapping showed the presence of C and O without any other impurities (Fig. S8†). ICP-MS results revealed the absence of other metallic impurities, signifying a purity of  $99 \pm 0.24\%$  for Li<sub>2</sub>CO<sub>3</sub>.

### Development of a ZLD process

After the recovery of lithium, the mother liquor was slightly coloured and was treated with recovered acetic acid for neutralization and activated charcoal for decolorization. The resultant mother liquor was concentrated to obtain sodium acetate as the only by-product. As the quantity of sodium acetate is in large excess compared to other salts, the remaining lithium and other unrecovered salts do not affect its purity drastically. The PXRD patterns of sodium acetate ascertained its crystalline nature (Fig. 5E). EDX elemental mapping showed the presence of Na, C, and O without any other impurities (Fig. S9†). ICP-MS results revealed the absence of other metallic impurities, signifying a purity of  $97 \pm 0.86\%$ . The recovery of the by-product is important in achieving a closed-loop process, which is along the lines of the present environmental norms. This also helps in improving the cost competitiveness of the process. However, such recovery of by-products to establish a zero-liquid discharge process has rarely been attempted, to our understanding.

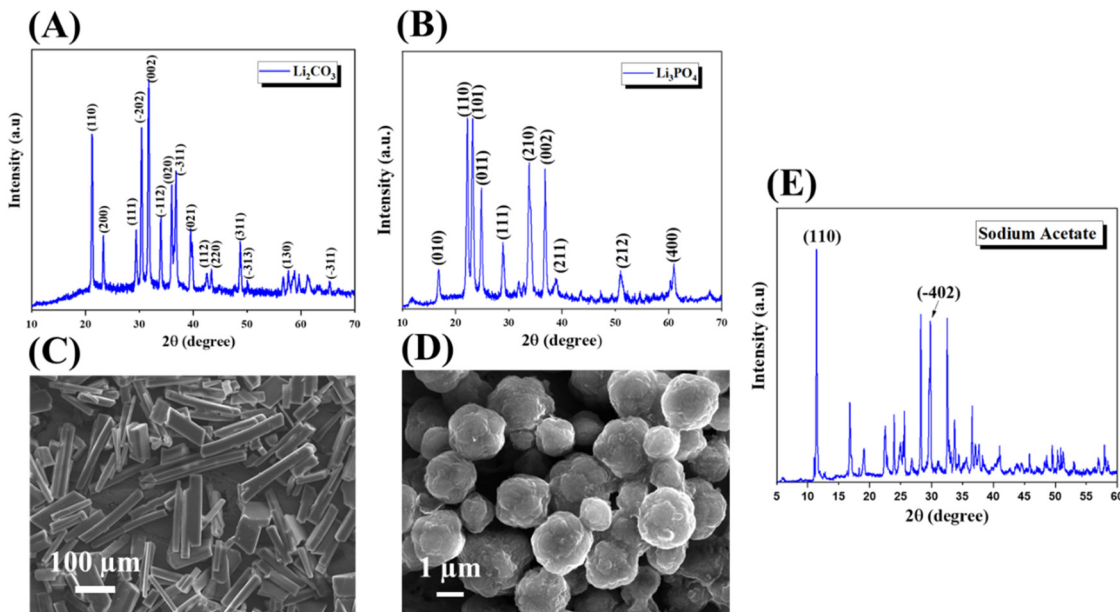


**Fig. 5** (A and B) Powder XRD of recovered pure  $\text{Li}_2\text{CO}_3$  and  $\text{Li}_3\text{PO}_4$ . (C and D) FE-SEM morphology of  $\text{Li}_2\text{CO}_3$  and  $\text{Li}_3\text{PO}_4$ . (E) Powder XRD of crystalline sodium acetate.

### Recycling of reagents

Since  $\text{Ni}(\text{DMG})_2$  complex has remained unexplored from the commercial standpoint, it was used as a precursor to synthesize a more conventional Ni complex under acidic conditions, subsequent to the recovery of the DMG ligand.<sup>58</sup>

Under the optimized reaction conditions, a 5% aq. HCl results in the dissociation of the  $\text{Ni}(\text{DMG})_2$  complex releasing water-insoluble dimethylglyoxime (DMG), while nickel remains in solution as nickel chloride. DMG was isolated and recrystallized. Following this, the nickel is isolated as  $\beta\text{-Ni(OH)}_2$  by treating it with sodium hydroxide (at a pH of  $\geq 11$ ) (Fig. 6).<sup>58</sup>

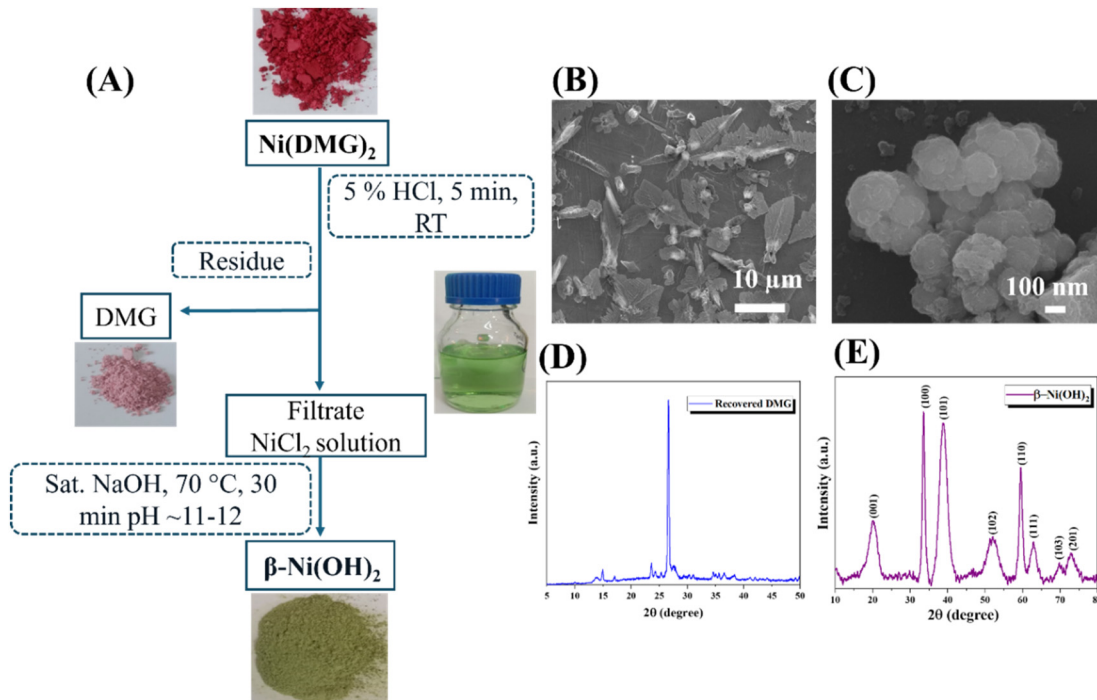


**Fig. 6** (A) The flowchart for the recovery of Ni and DMG from the spent LIB-derived  $\text{Ni}(\text{DMG})_2$  complex. (B and C) FE-SEM morphology of recovered DMG and  $\beta\text{-Ni(OH)}_2$ . (D and E) Powder XRD of recovered DMG and  $\beta\text{-Ni(OH)}_2$ .

The recovered DMG and  $\beta$ -Ni(OH)<sub>2</sub> were characterized using PXRD, SEM, FT-IR, and ICP-MS analyses to ascertain their properties and confirm their purity. The separated DMG was recycled/reused for subsequent recovery cycles to isolate the Ni(DMG)<sub>2</sub> complex from the leached liquor of spent LIBs.

### Recovery of valuable components from the spent anode of LIBs

The anode of a lithium-ion battery in smartphones is typically made up of graphite applied onto a copper foil surface. However, during the process of charging and discharging, lithium ions migrate between the anode and cathode through the electrolyte interface. Consequently, a small quantity of lithium is also present in the anode.<sup>59</sup> The initial composition of metals in the anode (1.06 wt% of Li, 0.0028 wt% of Co, 0.225 wt% of Mn, 0.0039 wt% of Ni, and 3.09 wt% of Cu) was determined *via* ICP-MS analysis (measured in weight percentage). For the leaching experiments, the entire calcined anode, comprising the copper foil with the anode material, was utilized. These experiments utilized acetic acid recovered from the leached liquor of spent cathode (concentration 1.7 M) with a pulp density of 100 g L<sup>-1</sup>, at a temperature of 75 °C, for a duration of 100 minutes. It was observed that metal leaching occurred concurrently with the separation of graphite from the copper foil. After filtration, the residue was dried and sieved to easily segregate the fine graphite powder from the copper foil (Fig. 7). Initial analysis of the leached solution showed a 96% leaching of lithium, with some copper also being leached from the copper foil, resulting in a bluish-colored solution. When the solvent was changed from acetic acid to water, the recovery rate of lithium decreased to approximately 71%. This obser-

vation indicates that the recovered acetic acid is highly effective in extracting lithium under optimized conditions. The pH of the leached solution was adjusted to around pH 6.5 by adding NaOH solution, causing Cu(OH)<sub>2</sub> to precipitate out (Fig. 7), which was subsequently filtered. After the recovery of copper, the trace amounts of Co, Ni, and Mn were precipitated and separated by adjusting the pH to around 10 with NaOH. Following this, a saturated solution of Na<sub>2</sub>CO<sub>3</sub> was added under boiling conditions to isolate lithium as Li<sub>2</sub>CO<sub>3</sub> (Fig. S10†). All the recovered materials (graphite powder, Cu(OH)<sub>2</sub>, and Li<sub>2</sub>CO<sub>3</sub>) were characterized to determine their identity and purity (Fig. 7).

### A closed-loop zero-liquid discharge process for metal recovery from spent LIBs

The principles of green chemistry are rarely applied in the mining of metals or during the recycling and recovery of metals from spent electronic wastes.<sup>20,60</sup> In consideration of the principles of green chemistry, an efficient process was designed to recover valuable metals from spent LIBs having mixed chemistries. A schematic representation of the process flow has been presented in (Fig. 8). After discharging and dismantling, the entire cathode along with the aluminium foil was treated with acetic acid with dropwise addition of 5% H<sub>2</sub>O<sub>2</sub>, which simultaneously leaches the cathode active material and separates them from the aluminium foil in a single-step operation without pretreatment steps to remove the PVDF binder. The leaching efficiency under optimized conditions is >98% for Li, Ni, Co, and Mn. The metals were then sequentially precipitated under a controlled pH to obtain the individual metal complexes in pure form *i.e.* Ni as Ni(DMG)<sub>2</sub>

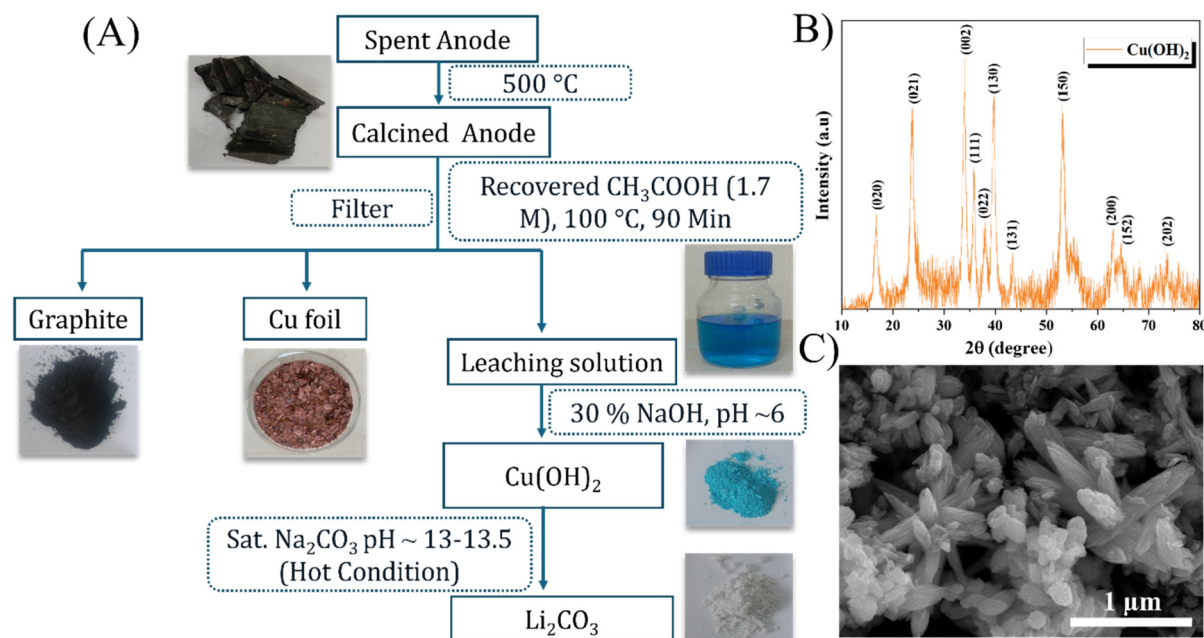
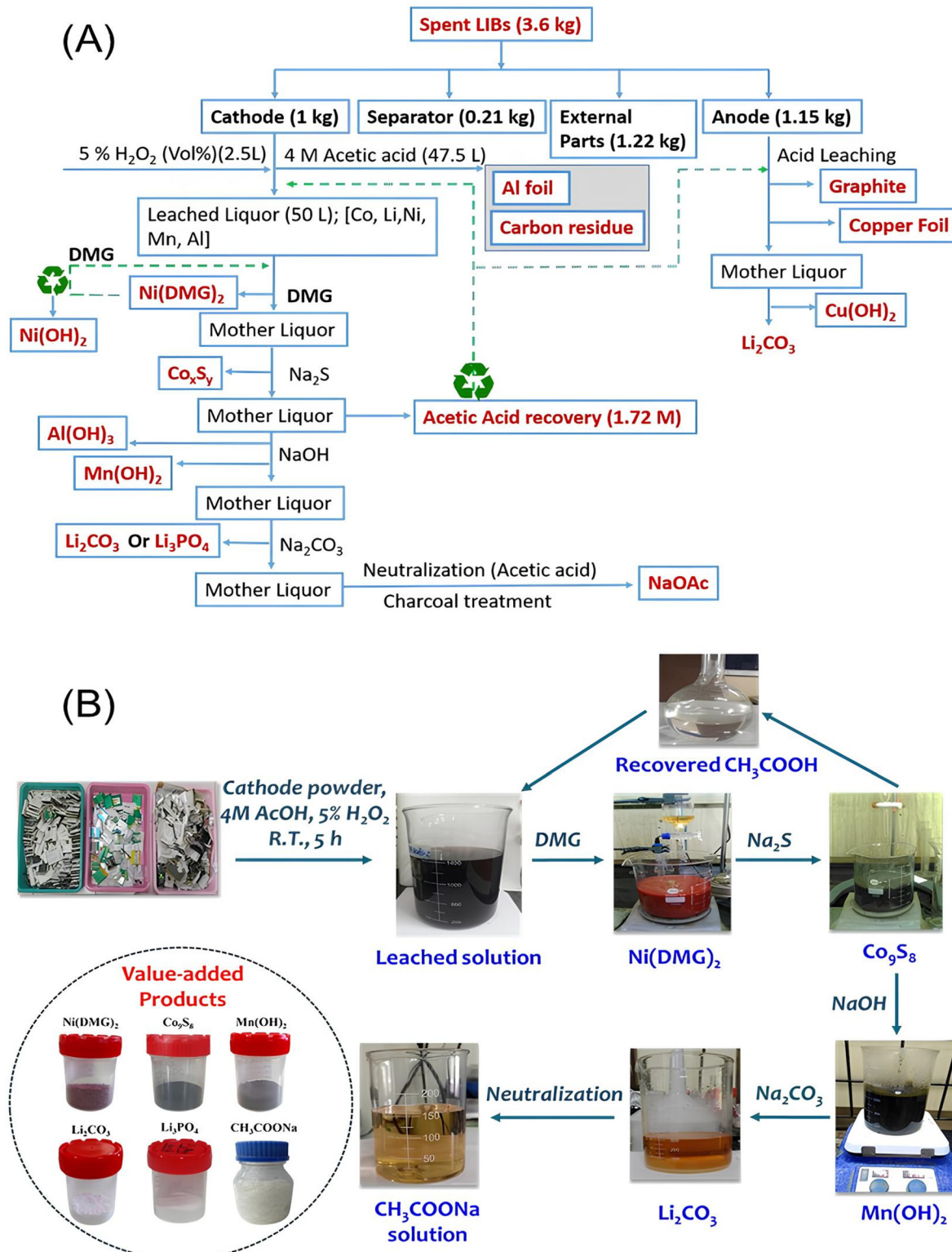


Fig. 7 (A) The flow chart for the recovery of metals and graphite from spent LIB anodes. (B) depicts the PXRD and (C) the FE-SEM of Cu(OH)<sub>2</sub> respectively.



**Fig. 8** (A) Flow sheet for a single batch of cathode and anode showing hydrometallurgical leaching & sequential chemical precipitation methods adopted in our studies using spent LIBs, and (B) digital images of the products recovered during the process.

and subsequently as  $\beta$ -Ni(OH)<sub>2</sub> after the recovery and recycling of DMG, Co as Co<sub>9</sub>S<sub>8</sub>, Mn as Mn(OH)<sub>2</sub> with a and Li as Li<sub>2</sub>CO<sub>3</sub> or Li<sub>3</sub>PO<sub>4</sub> respectively. Acetic acid was recycled in the process

and collected from the leached liquor by distillation. The concentration of the recovered acetic acid was 1.72 M, which was determined by titration with 1 M NaOH. The decrease in con-

centration of the acetic acid is due to its close boiling point with water (117.9 °C), which makes it difficult to avoid the presence of water in the distilled acetic acid. The remaining acetic acid/acetate in the system is recovered as sodium acetate ( $\text{CH}_3\text{COONa}$ ) in bulk at the end of the process, making this a zero-discharge process. The recycled acetic acid was subsequently used for the recovery of metals from the anode to recover graphite, copper foil, and  $\text{Li}_2\text{CO}_3$  separately. The distilled acetic acid can also be used in the recovery of metals from the cathode by increasing its concentration to 4 M by the addition of glacial acetic acid. The state-of-the-art solvents for leaching of metal ions from the cathode and anode are tabulated separately for comparison (Tables S1 & S2†). We also conducted a tentative economic analysis based on the mass balance for 3.6 kg of battery, which produces 1 kg of cathode material, showing that the process is profitable (Tables S3–S5†). It is essential to recognize that the composition of different batteries can vary, resulting in differences in mass balances and economic viability. Therefore, prioritizing the efficiency of extraction (ensuring complete recovery) and the purity of materials is crucial, alongside evaluating technoeconomic feasibility. Moreover, the environmental benefits of the recycling process should also be taken into account. In our process, the successful recovery of DMG is an added advantage, further substantiating the benefits of a metal extraction process by the selective precipitation of metals using a complexing reagent, followed by its facile recovery by de-chelation and reuse. This also aids in improving the cost competitiveness of the process. Thus, we propose a green and efficient metal leaching process from the entire cathode in the presence of acetic acid that precludes the necessity of heating or organic solvent-based pre-treatment steps to remove the PVDF binder. The recovery of individual metals was achieved through pH-controlled selective and sequential precipitation of the metals as their salts. Concomitantly, acetic acid was recovered and recycled by simple distillation, which can be used in both anode and cathode recycling. Finally, sodium acetate is recovered as sodium acetate (~97% purity). Thus, this process precludes the generation of any secondary waste and achieves a zero-liquid discharge closed-loop recycling of valuable metals present in spent LIBs. We have demonstrated the scalability of the process at a 1 kg scale. However, the main challenge lies in the pulp density ( $20 \text{ g L}^{-1}$ ), which needs to be enhanced, as it could impact the reactor sizing when scaling up.

## Experimental section

A standard procedure was followed for battery discharging before the manual dismantling of batteries to separate the cathode, anode, separator, and casing. This work involves two main experimental procedures, leaching of cathode & anode material and downstream processing of leached liquor for sequential selective precipitation. Details of the processes have been provided in the ESL.†

## Representative procedure for metal leaching from the cathode of spent LIBs

In a standard experiment, the cathode powder was introduced into a glass reactor vessel equipped with a reflux condenser and mechanical stirrer. Acetic acid was then added, followed by drop-wise addition of  $\text{H}_2\text{O}_2$  over several hours, using a peristaltic pump with continuous stirring at room temperature or elevated temperature, for different sets of experiments. Upon completion of the reaction, any undigested solid materials were separated using a nose filter and subsequently dried. The various leaching parameters were optimized (room temperature (30 °C), 20 g  $\text{L}^{-1}$  pulp density, 4 M acetic acid, 5 vol%  $\text{H}_2\text{O}_2$ , and time duration of 5 h) to get maximum leaching efficiency of >98%. After the leaching parameter optimization, a 1 kg batch of whole cathode (with Al foil; cut into 20 × 20 mm pieces) was used for leaching (total 50 L; 2.5 L  $\text{H}_2\text{O}_2$  & 47.5 L, 4 M acetic acid) studies and the leached liquor (composition: 0.86 g  $\text{L}^{-1}$  of Li, 5.02 g  $\text{L}^{-1}$  of Co, 1.06 g  $\text{L}^{-1}$  of Mn, 0.54 g  $\text{L}^{-1}$  of Ni, 0.45 g  $\text{L}^{-1}$  of Al) was processed in 1 L batches to optimize sequential and selective precipitation of Ni, Co, Al, Mn, Li, and the by-product sodium acetate. Details are provided in the ESL.†

## Conclusion

A closed-loop zero-liquid discharge process has been devised to extract all metals individually, from a mixed variety of used Lithium-Ion Batteries (LIBs) with high yield and purity. This is accomplished through a room-temperature hydrometallurgical leaching process followed by a pH-controlled sequential precipitation of individual metals as their salts. Unlike conventional methods that require a pre-treatment step to separate aluminum foil from the active cathode powder, our approach simultaneously leaches and separates the entire cathode, saving time, and energy, and eliminating potential hazards during large-scale industrial operations. The leaching process is conducted at room temperature, obviating the need for external heating, which in turn reduces the consumption of hydrogen peroxide due to its decomposition at higher temperatures, as it is an exothermic reaction, and diminishes the energy footprint of the process. Following the leaching process, metals are isolated through sequential chemical precipitation techniques. Achieving complete metal separation from NCM-type cathode material, which contains multiple metals, using precipitation-only route, highlights a key advantage over the typical approach that combines solvent extraction (for Ni and Co) with precipitation. This method not only diminishes fire risks but also reduces the number of steps involved while avoiding the use of solvent extraction techniques. Excess acetic acid is also reclaimed and reused in the processing of the anode for lithium recovery. The recycled  $\text{Ni}(\text{DMG})_2$  complex is utilized to retrieve DMG and nickel in a usable form. Ultimately, the process produces only one by-product, sodium acetate, leading to a zero-liquid discharge system. This minimizes waste generation and contributes to a

reduced environmental footprint. We have also demonstrated the processing of both cathode and anode materials, as well as the recycling of products as necessary from a commercial perspective. This entire process effectively addresses environmental pollution concerns and promotes a circular economy by recovering individual associated metals from used LIBs.

## Author contributions

Nishu Choudhary: methodology, investigation, formal analysis, writing – original draft. Hiren Jungi: methodology, investigation, visualization, writing-original draft. Maulik V. Gauswami: methodology, investigation, validation, writing – original draft. Anu Kumari: formal analysis, data curation, validation. Arvind B. Boricha: conceptualization, supervision, methodology. Jatin R. Chunawala: methodology, scale-up, resourcing. Joyee Mitra: conceptualization, supervision, methodology, writing – review & editing. Alok Ranjan Paital: conceptualization, funding acquisition, methodology, writing – review & editing. The manuscript was collaboratively written by all authors, and all have approved the final version.

## Data availability

The data supporting this article have been included as part of the ESI.†

## Conflicts of interest

The authors declare no conflict of interest.

## Acknowledgements

The authors are thankful to CSIR, New Delhi, India for funding under the CSIR Mission project on Bulk chemicals (WP-2: Extraction of Critical Metals from used Li-ion Batteries HCP0028). N. C. & H. J. acknowledge CSIR & AcSIR for fellowship & Ph.D. degree. AESD & CIF division of CSIR-CSMCRI is acknowledged for providing analytical facilities. A CSIR-CSMCRI communication no. 107/2024.

## References

- 1 H. Kopperi, V. Mamidi, G. Suresh and S. V. Mohan, *Green Chem.*, 2025, **27**, 2359–2373.
- 2 R. Hardian, A. Ghaffar, C. Shi, E. Y. X. Chen and G. Szekely, *J. Membr. Sci. Lett.*, 2024, **4**, 100067.
- 3 J. Lan, C. Deng, Z.-Y. Zhao and Y.-Z. Wang, *Green Chem.*, 2025, **27**, 1183–1193.
- 4 G. Harper, R. Sommerville, E. Kendrick, L. Driscoll, P. Slater, R. Stolkin, A. Walton, P. Christensen, O. Heidrich, S. Lambert, A. Abbott, K. Ryder, L. Gaines and P. Anderson, *Nature*, 2019, **575**, 75–86.
- 5 D. Di Lecce, R. Verrelli and J. Hassoun, *Green Chem.*, 2017, **19**, 3442–3467.
- 6 M. K. Tran, M.-T. F. Rodrigues, K. Kato, G. Babu and P. M. Ajayan, *Nat. Energy*, 2019, **4**, 339–345.
- 7 M. Chen, X. Ma, B. Chen, R. Arsenault, P. Karlson, N. Simon and Y. Wang, *Joule*, 2019, **3**, 2622–2646.
- 8 J. Hou, X. Ma, J. Fu, P. Vanaphuti, Z. Yao, Y. Liu, Z. Yang and Y. Wang, *Green Chem.*, 2022, **24**, 7049–7060.
- 9 X. Zhang, L. Li, E. Fan, Q. Xue, Y. Bian, F. Wu and R. Chen, *Chem. Soc. Rev.*, 2018, **47**, 7239–7302.
- 10 T. Raj, K. Chandrasekhar, A. N. Kumar, P. Sharma, A. Pandey, M. Jang, B. H. Jeon, S. Varjani and S. H. Kim, *J. Hazard. Mater.*, 2022, **429**, 128312.
- 11 Y. Zhang, W. Wang, J. Hu, T. Zhang and S. Xu, *ACS Sustainable Chem. Eng.*, 2020, **8**, 15496–15506.
- 12 P. Meshram, B. D. Pandey and T. R. Mankhand, *Hydrometallurgy*, 2014, **150**, 192–208.
- 13 H. Bae and Y. Kim, *Mater. Adv.*, 2021, **2**, 3234–3250.
- 14 X. Chen, J. Li, D. Kang, T. Zhou and H. Ma, *Green Chem.*, 2019, **21**, 6342–6352.
- 15 H. Jungi, A. A. Virani, S. Podder, H. Girase and J. Mitra, *Batteries Supercaps*, 2024, e202400518.
- 16 W. Lv, Z. Wang, H. Cao, Y. Sun, Y. Zhang and Z. Sun, *ACS Sustainable Chem. Eng.*, 2018, **6**, 1504–1521.
- 17 F. Larouche, F. Tedjar, K. Amouzegar, G. Houlachi, P. Bouchard, G. P. Demopoulos and K. Zaghib, *Materials*, 2020, **13**, 801.
- 18 Y. Li, W. Lv, H. Huang, W. Yan, X. Li, P. Ning, H. Cao and Z. Sun, *Green Chem.*, 2021, **23**, 6139–6171.
- 19 Y. Xu, Y. Dong, X. Han, X. Wang, Y. Wang, L. Jiao and H. Yuan, *ACS Sustainable Chem. Eng.*, 2015, **3**, 2435–2442.
- 20 Y. Yang, X. Meng, H. Cao, X. Lin, C. Liu, Y. Sun, Y. Zhang and Z. Sun, *Green Chem.*, 2018, **20**, 3121–3133.
- 21 M. K. Jha, A. Kumari, A. K. Jha, V. Kumar, J. Hait and B. D. Pandey, *Waste Manag.*, 2013, **33**, 1890–1897.
- 22 K. Wang, G. Zhang, M. Luo and J. Li, *Chem. Eng. J.*, 2023, **472**, 145006.
- 23 L. Li, E. Fan, Y. Guan, X. Zhang, Q. Xue, L. Wei, F. Wu and R. Chen, *ACS Sustainable Chem. Eng.*, 2017, **5**, 5224–5233.
- 24 Y. Chen, N. Liu, F. Hu, L. Ye, Y. Xi and S. Yang, *Waste Manag.*, 2018, **75**, 469–476.
- 25 Z. Cun, P. Xing, C. Wang, H. Li, S. Ma, Z. Sun, Q. Wang and X. Guan, *Resour., Conserv. Recycl.*, 2024, **202**, 107390.
- 26 R. Golmohammadzadeh, F. Faraji and F. Rashchi, *Resour., Conserv. Recycl.*, 2018, **136**, 418–435.
- 27 W. Gao, X. Zhang, X. Zheng, X. Lin, H. Cao, Y. Zhang and Z. Sun, *Environ. Sci. Technol.*, 2017, **51**, 1662–1669.
- 28 Y. Bai, R. Essehli, C. J. Jafta, K. M. Livingston and I. Belharouak, *ACS Sustainable Chem. Eng.*, 2021, **9**, 6048–6055.
- 29 T. Suzuki, T. Nakamura, Y. Inoue, M. Niinae and J. Shibata, *Sep. Purif. Technol.*, 2012, **98**, 396–401.
- 30 F. Wang, R. Sun, J. Xu, Z. Chen and M. Kang, *RSC Adv.*, 2016, **6**, 85303–85311.

31 X. Yang, Y. Zhang, Q. Meng, P. Dong, P. Ning and Q. Li, *RSC Adv.*, 2020, **11**, 268–277.

32 Z. Wang, Y. Chen, F. Zhou, R. Qin, Y. Tian, Z. Xue and T. Mu, *Green Chem.*, 2024, **26**, 5988–5996.

33 Y. Tian, F. Zhou, Z. Wang, W. Chen, R. Qin, Y. Chen and T. Mu, *Sep. Purif. Technol.*, 2024, **348**, 127810.

34 Y. Hu, M. Yang, Q. Dong, X. Zou, J. Yu, S. Guo and F. Yan, *Energy Environ. Sci.*, 2024, **17**, 4238–4247.

35 R. Chen, *J. Ionic Liq.*, 2023, **3**, 100070.

36 X. Wu, Z. Liu, H. Li, Z. Fu, G. Zhang, H. Zhang, G. Wang and Y. Zhang, *Sep. Purif. Technol.*, 2025, **354**, 128808.

37 M. J. Roldán-Ruiz, M. L. Ferrer, M. C. Gutiérrez and F. d. Monte, *ACS Sustainable Chem. Eng.*, 2020, **8**, 5437–5445.

38 H. Shi, Y. Luo, C. Yin and L. Ou, *Green Chem.*, 2024, **26**, 8100–8122.

39 S. S. de Jesus and R. M. Filho, *Renewable Sustainable Energy Rev.*, 2022, **157**, 112039.

40 C. J. Clarke, W. C. Tu, O. Levers, A. Brohl and J. P. Hallett, *Chem. Rev.*, 2018, **118**, 747–800.

41 Y. Li, J. Luo, S. Shan and Y. Cao, *J. Mol. Liq.*, 2023, **370**, 121044.

42 S. Lei, Y. Zhang, S. Song, R. Xu, W. Sun, S. Xu and Y. Yang, *ACS Sustainable Chem. Eng.*, 2021, **9**, 7053–7062.

43 C. M. Costa, J. C. Barbosa, R. Gonçalves, H. Castro, F. J. Del Campo and S. Lanceiros-Méndez, *Energy Storage Mater.*, 2021, **37**, 433–465.

44 G. P. Nayaka, Y. Zhang, P. Dong, D. Wang, Z. Zhou, J. Duan, X. Li, Y. Lin, Q. Meng, K. V. Pai, J. Manjanna and G. Santhosh, *J. Environ. Chem. Eng.*, 2019, **7**, 102854.

45 H. Jin, J. Zhang, D. Wang, Q. Jing, Y. Chen and C. Wang, *Green Chem.*, 2022, **24**, 152–162.

46 K. H. Chan, J. Anawati, M. Malik and G. Azimi, *ACS Sustainable Chem. Eng.*, 2021, **9**, 4398–4410.

47 S. Natarajan, A. B. Boricha and H. C. Bajaj, *Waste Manag.*, 2018, **77**, 455–465.

48 X. Chen, Y. Wang, S. Li, Y. Jiang, Y. Cao and X. Ma, *Chem. Eng. J.*, 2022, **434**, 134542.

49 X. Chang, M. Fan, C. F. Gu, W. H. He, Q. Meng, L. J. Wan and Y. G. Guo, *Angew. Chem., Int. Ed.*, 2022, **61**, e202202558.

50 Y. Qi, M. Wang, L. Yuan and X. Chen, *Chem. Eng. J.*, 2023, **466**, 143030.

51 S. Gu, L. Zhang, B. Fu, X. Wang and J. W. Ahn, *Chem. Eng. J.*, 2021, **420**, 127561.

52 X. Yin, Y. Wu, X. Tian, J. Yu, Y.-N. Zhang and T. Zuo, *ACS Sustainable Chem. Eng.*, 2016, **4**, 7080–7089.

53 B. Dönmez, F. Demir and O. Laçin, *J. Ind. Eng. Chem.*, 2009, **15**, 865–869.

54 S. S. Behera and P. K. Parhi, *Sep. Purif. Technol.*, 2016, **160**, 59–66.

55 Y.-W. Wang, *Process Saf. Environ. Prot.*, 2018, **113**, 122–131.

56 S. Gupta, K. K. Pant and G. Corder, *Chem. Eng. J.*, 2022, **446**, 137397.

57 J. Ma, W. Meng, L. Zhang, F. Li and T. Li, *RSC Adv.*, 2021, **11**, 5035–5043.

58 H. Jungi, A. Karmakar, S. Kundu and J. Mitra, *J. Mater. Chem. A*, 2023, **11**, 13687–13696.

59 Y. Guo, F. Li, H. Zhu, G. Li, J. Huang and W. He, *Waste Manag.*, 2016, **51**, 227–233.

60 R. M. Izatt, S. R. Izatt, N. E. Izatt, K. E. Krakowiak, R. L. Bruening and L. Navarro, *Green Chem.*, 2015, **17**, 2236–2245.